

1 *Applying computer vision to digitised natural history collections for climate change research:*
2 *temperature-size responses in British butterflies*

3

4 Rebecca J Wilson^{1,2*}, Alexandre Fioravante de Siqueira^{3*}, Stephen J Brooks², Benjamin W
5 Price², Lea M Simon¹, Stéfan J van der Walt³, Phillip B Fenberg^{1,2}

6

7

8 ¹School of Ocean and Earth Sciences

9 University of Southampton

10 Southampton

11 SO14 3ZH

12 UK

13

14 ²Department of Life Sciences

15 Natural History Museum

16 London

17 SW7 5BD

18 UK

19

20 ³Berkeley Institute for Data Science

21 University of California

22 Berkeley, CA

23 94720

24 USA

25

26 Corresponding author:

27 Phillip B Fenberg

28 p.b.fenberg@soton.ac.uk

29

30 * These authors contributed equally to the paper and share joint first-authorship

31

32 Running head: Computer vision and natural history collections

33 ABSTRACT

34

35 1. Natural history collections (NHCs) are invaluable resources for understanding biotic
36 response to global change. Museums around the world are currently imaging
37 specimens, capturing specimen data, and making them freely available online. In
38 parallel to the digitisation effort, there have been great advancements in computer
39 vision (CV): the computer trained automated recognition/detection, and
40 measurement of features in digital images. Applying CV to digitised NHCs has the
41 potential to greatly accelerate the use of NHCs for biotic response to global change
42 research. In this paper, we apply CV to a very large, digitised collection to test
43 hypotheses in an established area of biotic response to climate change research:
44 temperature-size responses.

45 2. We develop a CV pipeline (Mothra) and apply it to the NHM iCollections of British
46 butterflies (>180,000 specimens). Mothra automatically detects the specimen in the
47 image, sets the scale, measures wing features (e.g., forewing length), determines the
48 orientation of the specimen (pinned ventrally or dorsally), and identifies the sex. We
49 pair these measurements and meta-data with temperature records to test how adult
50 size varies with temperature during the immature stages of species and to assess
51 patterns of sexual-size dimorphism across species and families.

52 3. Mothra accurately measures the forewing lengths of butterfly specimens and
53 compared to manual baseline measurements, Mothra accurately determines sex and
54 forewing lengths of butterfly specimens. Females are the larger sex in most species
55 and an increase in adult body size with warm monthly temperatures during the late
56 larval stages is the most common temperature size response. These results confirm

57 suspected patterns and support hypotheses based on recent studies using a smaller
58 dataset of manually measured specimens.

59 4. We show that CV can be a powerful tool to efficiently and accurately extract
60 phenotypic data from a very large collection of digital NHCs. In the future, CV will
61 become widely applied to digital NHC collections to advance ecological and
62 evolutionary research and to accelerate the use of NHCs for biotic response to global
63 change research.

64

65

66 KEYWORDS Butterfly, Computer vision, Climate Change, Deep Learning, digitisation,

67 Lepidoptera, Mothra, Natural History Collections

68

69 1 INTRODUCTION

70

71 The world's natural history collections contain at least two billion specimens (Ariño 2010).
72 Tens of millions of these specimens (and counting) are making their way out of the halls and
73 cabinets of natural history museums and into the virtual world as digital images and
74 specimen data, either through data portals (<https://data.nhm.ac.uk/>) or aggregators (e.g.,
75 <https://www.gbif.org/>) (Nelson & Ellis 2019). The purpose of this vast effort is two-fold: to
76 provide a digital copy of these priceless collections and to advance the core research of
77 museums for understanding the history and biodiversity of the living world. But as the
78 Anthropocene progresses, digitised natural history collections (NHCs) can also be leveraged
79 for understanding the biological impacts of global change (Johnson *et al.* 2011; Meineke *et*
80 *al.* 2019). Not only will the widespread availability of specimen images and data increase the
81 rate at which scientists can perform this essential research, but the sheer taxonomic, spatial
82 and temporal scope of digitised NHCs will help provide a more holistic understanding of how
83 the biosphere has and will respond to global change.

84

85 Digitised NHCs have been used to investigate multiple aspects of biotic response to global
86 change, including documenting changes in geographic range and biodiversity (Kharouba *et*
87 *al.* 2019; Ewers-Saucedo *et al.* 2021), phenology (Brooks *et al.* 2017), and body size of
88 species (Wilson *et al.* 2019; Wonglersak *et al.* 2020). While such studies are incredibly
89 important, the number of specimens used are often limited due to the time required to
90 physically measure and record each specimen. For example, until recently, studies
91 examining change in body size using images must first open images in software, set the
92 scale, and manually measure body size or its proxies (Fenberg *et al.* 2016). Thus, despite

93 their availability, specimen images still require time-consuming manipulation and manual
94 measurement - limiting the amount of data available for individual research projects.

95

96 In parallel to mass digitisation efforts by museums, major advancements have been made in
97 computer vision (CV) technologies. CV is a rapidly developing field in which computers are
98 trained to recognise, extract and measure information from digital images or video. While
99 practical applications of CV have been made in several fields, such as object
100 recognition/detection for medical purposes (e.g., tumor detection; Svoboda 2020) and
101 ecologists are starting to use CV for biodiversity analyses in the field (Bjerger *et al.* 2021), CV
102 is only starting to be used for ecology and evolution research.

103

104 Given the rapid advancements in CV technology and its many applications, it is thought that
105 CV will become an essential tool for ecology and evolutionary biologists (Lürig *et al.* 2021).

106 For example, CV can be used along with molecular data to help identify cryptic species and
107 other eco-evolutionary questions (Høye *et al.* 2021). Currently however, there are very few
108 studies showcasing the powerful utility of pairing CV with NHCs for the purposes of climate
109 change research (Hsiang *et al.* 2019; McAllister *et al.* 2019). In this paper, we apply CV to a
110 very large, digitised collection to test hypotheses in an established area of biotic response to
111 climate change research: temperature-size responses (Sheridan & Bickford 2011).

112

113 1.1 Temperature-size responses

114

115 Body size is one of the most important traits of an organism due to its correlation with many
116 aspects of the life history, ecology, and evolution of species. However, climate warming is

117 thought to be causing widespread reduction in body size and is even suggested to be a
118 “universal” response to warming (Sheridan & Bickford 2011). However, recent studies show
119 that species can have varying responses (Horne *et al.* 2015; Tseng *et al.* 2018; Wonglersak *et*
120 *al.* 2020). This is especially true for insects, which, due to their complex and diverse life
121 cycles, can lead to a variety of temperature-size responses. Each life stage of
122 holometabolous insects can experience different environmental conditions, which may
123 cause each stage to respond in a different way to temperature (Kingsolver *et al.* 2011;
124 Wilson *et al.* 2019). In addition, each sex may have different temperature-size responses,
125 which may affect the magnitude of sexual size dimorphism (Fenberg *et al.* 2016). Thus, it is
126 important that life stages, sex, and the environmental conditions experienced by them, are
127 considered when investigating temperature-size responses.

128

129 Lepidoptera are useful study taxa for examining temperature-size responses as their life
130 stages are clearly defined, the sexes of many species can be easily identified, and they have
131 relatively short generation times. If adult body size measurements are paired with
132 temperature records across multiple generations, years, per sex, and for each immature life
133 stage (e.g., early to late larval and pupal stages), then it is possible to determine the
134 direction and strength of adult body size responses to temperature and which factors are
135 most predictive of observed responses (Bowden *et al.* 2015; Davies 2019).

136

137 NHCs paired with temperature records can provide a useful resource for studying
138 temperature-size responses because NHCs often span many decades, over which a large
139 range of inter- and intra-annual (i.e., seasonal) temperature records may be available. In
140 recent years, the use of NHCs to study temperature-size responses in insects has become

141 common, but responses often vary among taxa (Baar *et al.* 2018; Tseng *et al.* 2018). For
142 example, the body sizes of Zygoptera (damselflies) are more sensitive to temperature than
143 Anisoptera (dragonflies) (Wonglersak *et al.* 2020). This suggests that, at least in some insect
144 groups, phylogenetic relationships are also an important predictor of the direction and
145 magnitude of temperature-size responses. Butterflies often increase in adult size with
146 increasing temperature (MacLean *et al.* 2016) and analysis of four UK butterfly species
147 found that the strongest prediction of adult size was temperature during the late larval
148 stage (Fenberg *et al.* 2016; Wilson *et al.* 2019). But in order to determine if these are
149 general responses, more species and specimens need to be analysed.

150

151 Here, we use a newly developed CV pipeline to automatically measure body size attributes
152 (e.g., wing lengths), orientation (pinned ventrally or dorsally), and identify the sex of
153 specimens of British butterfly specimens housed at the NHM (n=184,533). We test the
154 accuracy of the pipeline by comparing the automated results to manual measurements of
155 30 butterfly species. We also test if there are patterns of sexual size dimorphism (SSD)
156 across 32 species, testing the hypothesis that females are larger than males (Teder 2014).

157

158 For temperature-size responses, we pair wing-length measurements with monthly
159 temperature records experienced by the immature stages of 24 species across four families
160 to determine the direction and strength of responses per species and to look for general
161 patterns across species. We hypothesise that the adult sizes of univoltine species (and first
162 generations of bivoltine species) will increase with increasing temperatures during the late
163 larval stages, and that males and females will respond differently, based on previous work
164 (Fenberg *et al.* 2016; Wilson *et al.* 2019). These same studies, however, also show that

165 increasing temperatures during the early larval stage causes some species to become
166 smaller as adults and that response to temperature during the pupal stages varies. We
167 therefore hypothesise that (i) warmer temperatures during the late larval stages will be
168 correlated with larger adults, (ii) warmer temperatures during early and pupal stages will
169 result in variable responses across species, and (iii), sex and family will be important factors
170 given recent studies (Wilson *et al.* 2019; Wonglersak *et al.* 2020).

171

172 1.2 Study system

173

174 The British butterfly specimens housed at the Natural History Museum (London) were
175 among the first very large scientific collections to be mass digitised. 184,533 specimens
176 comprising 94 species of butterflies (collected from 1803-2006) have been digitised during
177 the iCollections project (Paterson *et al.* 2016). Each pinned specimen is imaged with a scale
178 bar (mm) and associated labels. All specimen data have been extracted and databased for
179 specimens with sufficient information, which include the geo-referenced location, date of
180 collection, and collector. We use these data and life history information paired with
181 historical temperature records in order to test our temperature-size hypotheses.

182

183 2 METHODS

184

185 2.1 Mothra development

186

187 Mothra is a Python package for analysing images of Lepidoptera specimens, inferring sex
188 and measuring body size attributes using a combination of deep learning and image

189 processing techniques. It is built on NumPy (Harris *et al.* 2020), SciPy (Virtanen *et al.* 2020),
190 matplotlib (Hunter 2007), scikit-image (Van der Walt *et al.* 2014), PyTorch (Paszke *et al.*
191 2019), and fastai (Howard & Gugger 2020). Mothra processes images that include: the
192 pinned specimen, a scale bar, and several printed or hand-written labels (Fig. 1A). Mothra
193 identifies these image elements, finds key points on the specimen, makes measurements,
194 and translates pixel distances to millimetres after interpreting the scale bar. Mothra can be
195 applied to any images of pinned Lepidoptera specimens if a millimetre scale bar is present
196 (Fig. 1A) and can be trained to identify other scale bars as needed. While Mothra also works
197 on many moth species, we focus on butterflies for this paper as they were used to train the
198 segmentation algorithm.

199

200 To recognize image elements (specimen, scale, and labels), we use a U-Net convolutional
201 neural network (Ronneberger *et al.* 2015) with ResNet-34 (He *et al.* 2016) in the analysis
202 path (Zhang *et al.* 2018; Paszke *et al.* 2019; Howard & Gugger 2020). The ResNet-34
203 implementation from PyTorch is pre-trained on the ImageNet image database (Deng *et al.*
204 2009). The U-Net is trained using 150 manually segmented images of different Lepidoptera
205 species. Labels correspond to the three elements (specimen, scale, labels) as well as the
206 background. Each iteration of training uses a batch of four images, and training completes
207 after 26 epochs (i.e., after all data has been seen 26 times).

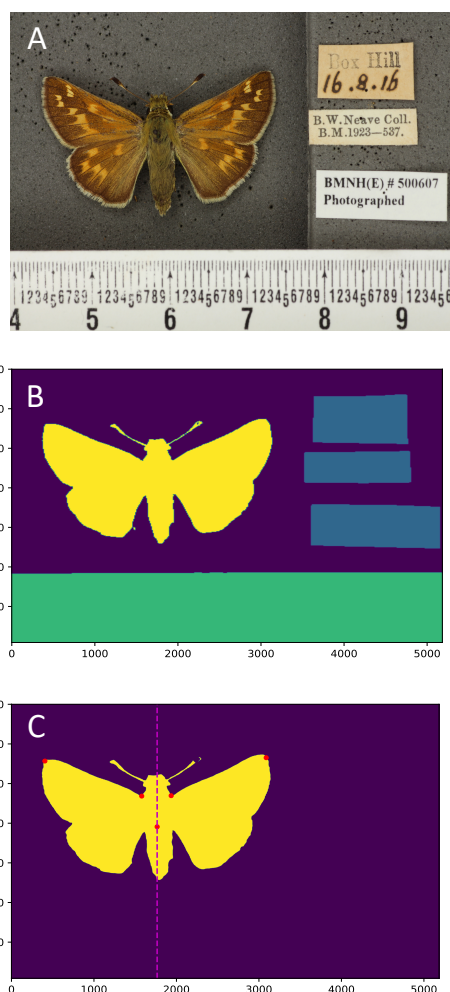
208

209 The network is trained using the 1cycle policy (Smith 2018), whereby learning rates start
210 low, increase, then drop back to below the initial value. The first epoch only trains the last
211 U-Net layer (bottom of the "U") with a learning rate of 2×10^{-3} while the rest of the
212 network is frozen. In subsequent epochs, the entire network is unfrozen. We use a

213 discriminative learning rate (i.e., a different learning rate for each layer; Smith 2018) of 10^{-5}
214 5 for the first layer, 10^{-3} for the last layer, and logarithmically interpolated values for the
215 middle layers. Training continues for a further 25 epochs.

216

217 The input dataset is augmented by changes in orientation, scale, exposure, and warp. Input
218 and labelled images were resized from their original size, 5184 x 3456 pixels, to 448 x 448
219 pixels. After classification, Mothra returns an image with labels corresponding to four
220 classes: specimen, scale bar (scale), labels, and background (Figure 1B). The central axis of
221 the specimen is taken as the horizontal centre of gravity. The image is then split into left and
222 right sides. Wing tips and shoulders are located (Figure 1C) for each side: the wing tip is
223 defined as the most distant pixel from the centre of the specimen, while the shoulder is
224 where the upper-central part of the body dips lowest in the vertical direction.



225

226 FIGURE 1. A.) Example input image (female *Hesperia comma*) containing the pinned

227 specimen, a scale bar, and data labels. B.) Image returned by Mothra, containing predictions

228 to the specimen (yellow), scale bar (green), labels (blue), and background (purple). C.) Wing

229 tips, shoulders, and centre (red dots) of the specimen (yellow). These points are used for the

230 measurements of forewing lengths (shoulders to wingtips), wingspan (wingtip to wingtip),

231 centre to wingtips, and shoulder width (shoulder to shoulder). Axis values in B and C are

232 pixel numbers.

233

234 To convert between pixel distances and millimetres, the scale bar is analysed. Its image

235 coordinates are returned by the classification step, after which the scale bar image is

236 extracted and turned into a binary image using an automated Otsu threshold (Otsu 1979).
237 Numbers are removed by filtering objects on their area and eccentricity, and the image is
238 then summed vertically to produce a one-dimensional vector of values. Summing across the
239 scale bar increases robustness against noise. That summation is, in turn, thresholded, since
240 we are only interested in transition periods, not in amplitudes. A Fast Fourier Transform is
241 then performed to determine the most dominant frequency. This frequency is given in
242 pixels per cycle and corresponds to the minor ticks on the scale bar: using it, we can convert
243 the measurements from pixels to millimetres.

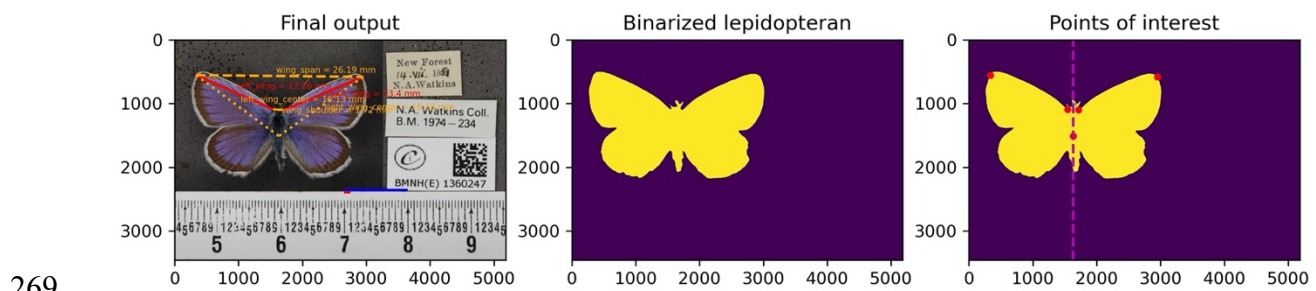
244

245 Next, we want to predict sex and orientation: either the specimen is pinned dorsally (with
246 the upper surface of the wings shown), or ventrally (with the underside of the wings
247 shown). For that purpose, we trained a ResNet-50 network using 2986 images separated
248 into three classes: 1549 pinned ventrally (where we did not classify sex), 722 male, and 715
249 female (both latter classes being pinned dorsally). Training images were resampled to 256 x
250 256 pixels, and data augmentation was performed using the Albumentations library
251 (Buslaev *et al.* 2020) which adds random changes of hue, saturation, and value in the
252 interval (-0.2, 0.2), as well as coarse dropout of rectangular regions in the image (DeVries &
253 Taylor 2017). Each augmentation was applied with a probability of 0.5 per generated
254 augmented sample.

255

256 Mothra, the collection of algorithms and functions implemented for this study, is
257 permissively licensed under the BSD-3 clause license and available on GitHub (Mothra Team,
258 2021). Mothra automatically downloads the latest pre-trained version of the neural
259 network. The data accompanying this study, including networks trained and images used in

260 training, are available on GitLab (Mothra Team, 2020). The images we used are part of the
261 iCollections project, released under the CC-BY license (Wilson *et al.*, 2020).
262
263 For each analysis Mothra takes an input folder of images or a text file listing the location of
264 the input images, and then outputs the following data as a CSV file: length (mm) of each
265 forewing, distance from each wing tip to the centre of the specimen (mm), wingspan from
266 wing tip to wing tip (mm), shoulder width between shoulders (mm), pinned orientation, and
267 sex. For each image an output image can be provided with the measurements overlaid (Fig.
268 2).



270 FIGURE 2. Example Mothra output image (male *Plebejus argus*) with the final output
271 showing the measurements overlaid on the image, the binarized specimen, and the points
272 of interest.

273

274 2.2 Mothra testing: manual versus automated measurements and sex ID

275

276 We manually measured the forewing lengths of 3,145 specimens of 30 species across four
277 families using ImageJ software. Measurements of four species are from previously published
278 research by the co-authors (Fenberg *et al.* 2016; Wilson *et al.* 2019). We then measured the
279 same specimens using Mothra. For each specimen, we calculated the average between the
280 left and right forewing lengths for both the manual and Mothra measurements. We then
281 compared the correlation between measurements across all specimens; testing if the slope
282 is equal to 1 (i.e., a one-to-one correlation). We also performed t-tests of measurements
283 grouped per family to test if the manual versus automated measurements are statistically
284 different. We categorised specimens by sex for species in which the sexes are reliably
285 detectable by eye from images (n=20 species; 2,807 specimens). A further 5,127 specimens
286 were identified to sex by Wilson (2021). We then compared the sex IDs for all specimens
287 combined (n=8,272 specimens from 20 species) to the Mothra outputs to determine the
288 accuracy of the automated sex identifications.

289

290 2.3 Mothra measurements of the iCollections

291

292 Once we determined the accuracy of the automated wing-length measurements and sex
293 identification (see below), we ran Mothra on all butterfly specimens within the iCollections
294 dataset (Paterson *et al.* 2016) using the NHM HPC cluster. This dataset constitutes 184,533
295 specimens. For analysis purposes, we only focus on the four main families that constitute
296 99% of the collections (Hesperiidae, Lycaenidae, Nymphalidae, Pieridae) and removed

297 species (n=32) which have either very few specimens (<100) or are not native to Britain
298 (e.g., rare occurrences). Ventrally pinned specimens (n=51,646) were removed to keep
299 forewing length measurements and sex identification consistent. Measurements of forewing
300 length for 130,173 specimens across 60 species and four families were analysed. For each
301 species, we removed any specimens in which the absolute value difference between the
302 right and left forewing lengths were larger than 2mm in order to remove any specimens
303 with wing damage. We also removed specimens for which the Mothra measurements were
304 clearly incorrect (e.g., measurements that were too large or small given the size of the
305 species) by examining the output images for the biggest outliers. We also checked the
306 remaining output images for the largest and smallest individuals per species to determine if
307 they were incorrect measurements. In total, only 1.8% of specimens were removed as clear
308 outliers/incorrect measurements (n=2,360), leaving 127,813 specimens for analysis (SI Table
309 2). For species which we trained Mothra for sex identification, we tested the hypothesis that
310 females are, on average, larger than males and looked for patterns across families.

311

312 2.4 Temperature-size responses: individual species analysis

313

314 We analysed a subset of the Mothra measurements for temperature-size responses (24
315 species). These species were chosen as they have good meta-data, are representative of
316 each family, and have varying life histories and habitat requirements. We only included
317 specimens if there was a known year, location, and month of collection, and collected on
318 the island of Great Britain. Where applicable, we separated specimens into generations (see
319 Wilson *et al.* 2019). If a species had a partial second generation, or a variable number of
320 generations from year to year, specimens were removed to keep the number of generations

321 per year consistent. For example, *Aglais urticae* has one generation in Scotland and two
322 generations a year in other parts of the UK, so Scottish specimens were removed.
323 Additionally, we removed specimens with collection dates outside the expected range of
324 adult flight season for that species, based on Thomas & Lewington (2014). We did not
325 include specimens of a species if there were fewer than three specimens available per year
326 (and sex where applicable). We used information about the life cycles of each species given
327 in Thomas & Lewington (2014) to determine which monthly temperatures were appropriate
328 for analyses. We used temperatures from months when species were in the early larval, late
329 larval and pupal stages; winter months were not used as growth would be limited. We used
330 mean monthly temperature data from the Central England Temperature Record for all
331 analyses (<https://www.metoffice.gov.uk/hadobs/hadcet/>).

332

333 Following Fenberg *et al.* (2016) and Wilson *et al.* (2019), we compared average forewing
334 length to average monthly temperatures using multiple linear regression analyses to
335 determine if temperatures experienced during the immature stages affect adult size. We
336 used R statistical packages MASS and MuMIn to run stepwise regression in both directions
337 to select variables for the final model and information theoretic (IT) model selection with
338 model averaging based on Akaike Information Criterion (AIC). Where applicable, we ran
339 separate models for each sex and generation.

340

341 A total of 17,727 specimens and 24 species are in the final analysis. In 15 species, males and
342 females could be identified, and three species had two generations that could be analysed
343 separately, giving a total of 44 models. For each species with a significant model, we
344 calculated the percentage change in adult size per °C for the most significant month in early

345 larval, late larval and pupal stages. Where there was not a significant variable for a
346 particular life stage, the most important non-significant variable was used. We calculated
347 percentage changes from slopes of the natural log of average forewing length versus
348 temperature: $((\exp(\text{slope})-1) \times 100)$.

349

350 2.5 Temperature-size responses: multi-species analysis

351

352 We compiled data to look for general patterns of temperature-size responses across
353 species. Firstly, we compiled the percentage change in adult size per °C of the three
354 immature stages for each species and, where applicable, each sex and generation. Secondly,
355 we compiled the natural log of average forewing lengths for all specimens used in the
356 individual species analyses. Natural logs were used to allow for species of different sizes to
357 be compared without the effects of scaling. We used temperature data from the most
358 important month for predicting adult size during each immature stage for the multi-species
359 analyses. We also included four other variables (family, habitat, size category, overwintering
360 stage) in the form of multi-level factors (SI Table 1) to determine which may affect the
361 strength and direction of temperature-size responses. We selected these four factor
362 variables a priori as likely having an influence on temperature-size response based on
363 previous research (Fenberg *et al.* 2016; Tseng *et al.* 2018; Davies 2019; Wilson *et al.* 2019).

364

365 We compared percentage change in adult size per °C increase in temperature during each
366 immature stage between the four factor variables (SI Table 1). We performed linear mixed
367 effects models using the natural log of average forewing lengths of specimens from all 24
368 species, with temperature during the early larval, late larval and pupal stages as fixed effects

369 and the random effects of family, overwintering stage, habitat and size category in each
370 model. ANOVAs and AIC values were used to determine which model gave the best fit. We
371 repeated analyses for species where sex could be determined, with sex included as a
372 random factor.

373

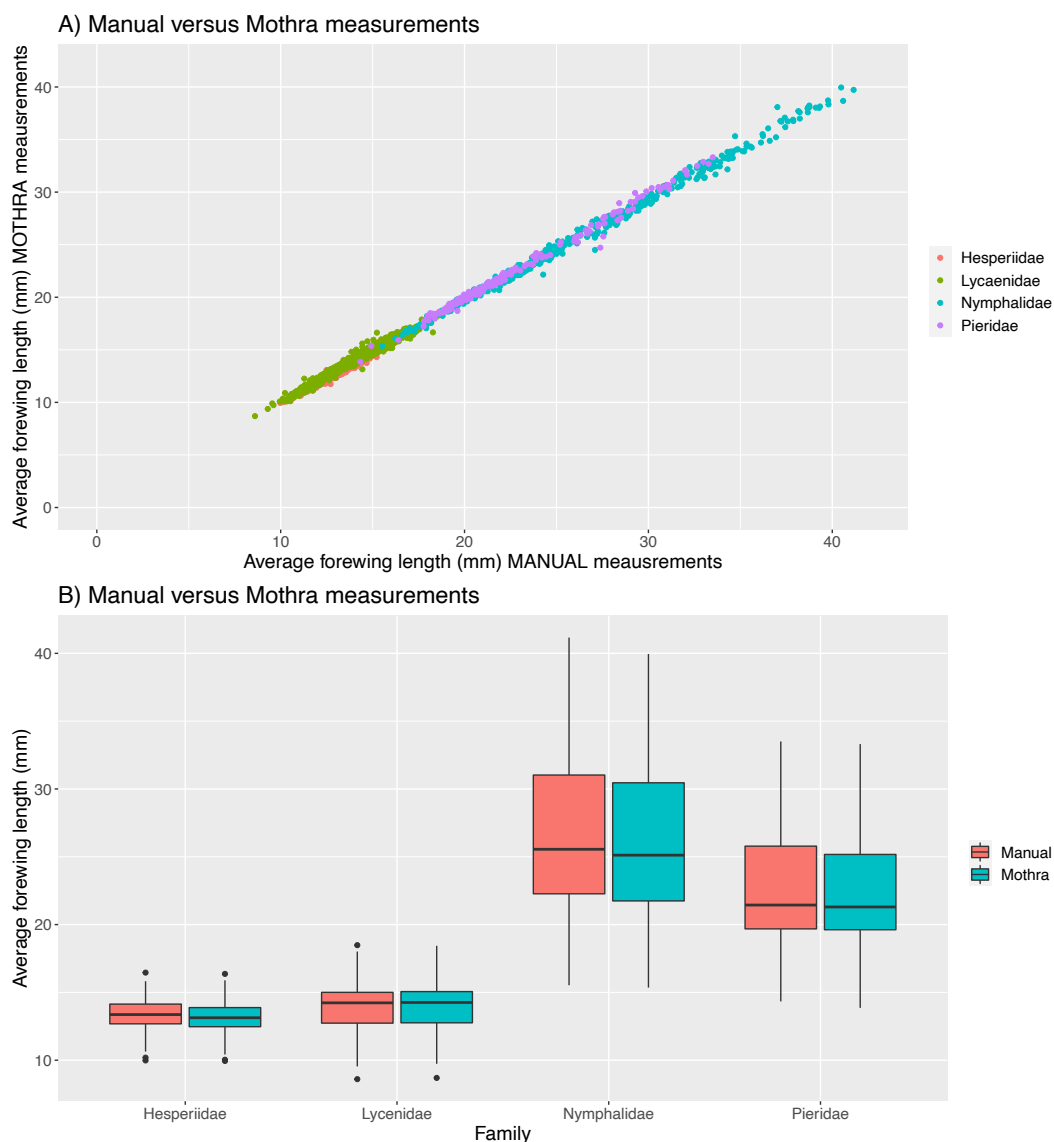
374 3 RESULTS

375

376 3.1 Automated versus manual measurements and sex ID

377

378 The Mothra measurements are nearly identical to the manual measurements (Fig. 3). The
379 correlation between average forewing length of the Mothra versus manual measurements is
380 0.98 and the slope is 1.0. After 6 clear outliers were removed, the correlation is 0.99 with a
381 slope of 1.03. These results indicate that there is a nearly perfect one-to-one relationship
382 between the Mothra and manual measurements. For all specimens combined, there is no
383 difference between measurements (t test, $P=0.33$). When grouped by family, manual versus
384 Mothra measurements are not statistically different except for HesperIIDae, where there is a
385 slight difference ($P<0.001$) in mean forewing length between manual (13.34 mm) and
386 Mothra measurements (13.12 mm). These differences are driven by *Hesperia comma*, due
387 to a consistent difference in where the wingtip was manually located by (Fenberg *et al.*
388 2016).



389
390 FIGURE 3. A.) Correlation between Mothra versus manual measurements for 3,145
391 specimens across 30 species from four families. Pearson's correlation $R = 0.99$ and the slope
392 = 1.03, revealing a nearly one to one relationship between manual and automated
393 measurements. B.) Boxplots comparing the manual versus automated measurements
394 grouped by family. Except for Heperiidae (see main text), there are no significant differences
395 between the two measurements. Six outliers were removed from these figures due to
396 incorrect Mothra measurements (see main text).

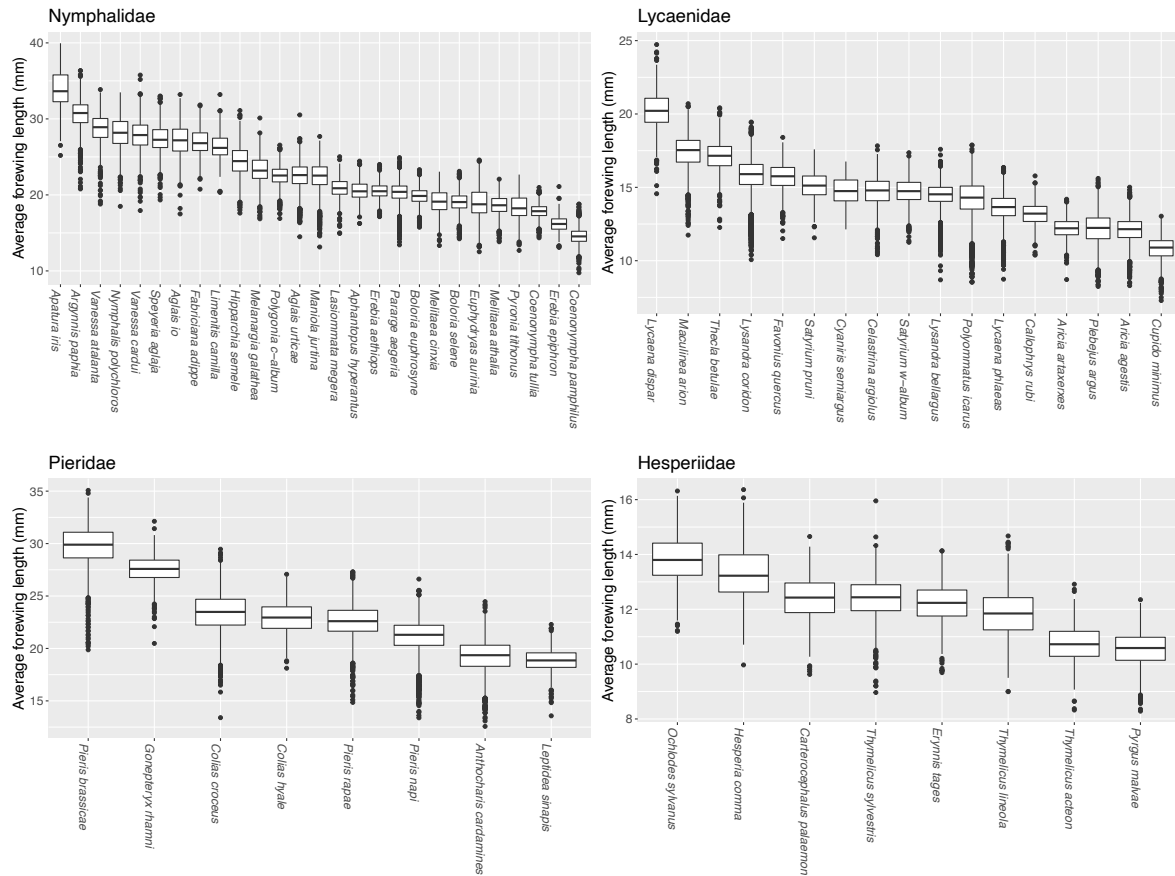
397 The sex identifications for species in which the sexes are reliably detectable by eye (n=20)
398 were highly accurate. Out of 5,127 specimens, only 2.9% (n=149 specimens) were different
399 between the manual versus Mothra identifications. After inspection of a subset specimens
400 that have a discrepancy in sex ID (n=41 specimens), it was noted that 17 specimens were
401 mis-identified by eye and 9 were misidentified by Mothra, the remaining 24 specimens were
402 discoloured or gynandromorphs where sex ID is not possible.

403

404 3.2 Size distribution and patterns of sexual size dimorphism

405

406 Given the accuracy of the wing length measurements and the sex identifications, we felt
407 confident to run Mothra on all specimens in the iCollections dataset (all results available
408 here: <https://doi.org/10.5281/zenodo.5759759> [embargoed until publication]; Price and
409 Fenberg 2021). The number of inaccurate measurements (either damaged specimens or
410 incorrect Mothra measurements) removed from the dataset was very small (1.8% of
411 specimens, see above), with the resulting size distributions per species seen in Figure 4. As
412 an initial test of the utility of this massive dataset, we tested the hypothesis that females are
413 larger than males per species (as is the case for many insect species, largely due to their
414 longer developmental times (Teder 2014). Our results show that this is broadly true for
415 British butterflies (Fig. 5). Out of 32 species, 30 have significant SSD, but males are the larger
416 sex in only seven species (five are in Lycaenidae and two in Pieridae; SI Table 2). Four of the
417 Lycaenidae are in the subfamily Polyommatainae (i.e., the blues). For the remaining species
418 (n=23), the females are the larger sex, including all species in HesperIIDae and Nymphalidae.



419

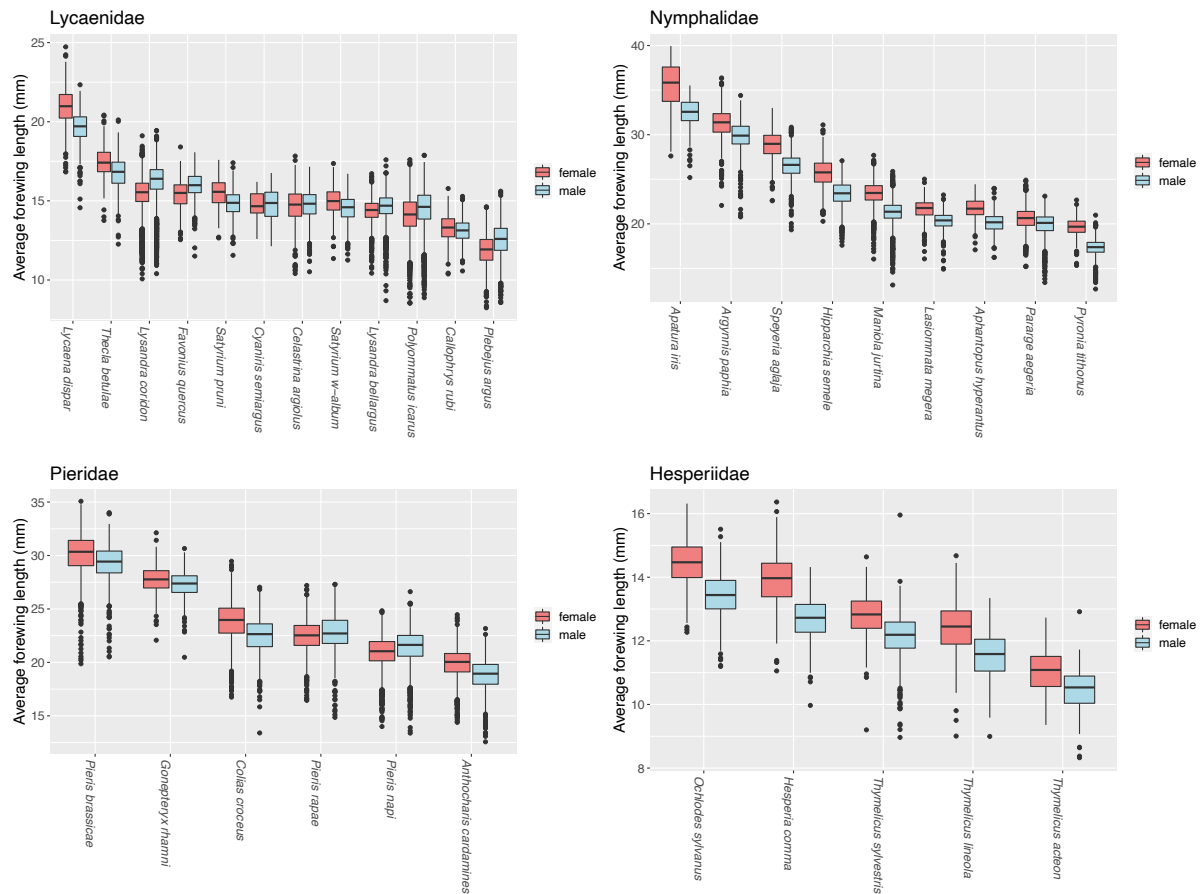
420 FIGURE 4. Size-distributions of the Mothra measurements of the dorsally pinned specimens

421 for each species in the iCollections native to the island of Great Britain from the four main

422 families (60 species). This figure represents measurements from a total of 127,813

423 specimens, excluding faulty measurements and damaged specimens (n=2,360 specimens).

424



425

426 FIGURE 5. Size distributions of the Mothra measurements for each species trained for sex

427 identification (n=32 species). Most species (n=23) have female biased sexual size

428 dimorphism (including all species in Hesperidae and Nymphalidae). Seven species have

429 male biased sexual size dimorphism (five species in Lycaenidae and two species in Pieridae)

430 and two species do not have sexual size-dimorphism.

431

432 3.3 Temperature-size responses: individual species analysis

433

434 When average forewing lengths were compared to monthly temperatures using multiple

435 linear regression models, 20 of the 44 models were significant. This accounted for 17 of the

436 24 species analysed. In all but four of the significant models, an increase in adult size with

437 increasing temperature during the late larval stage was significant. The responses of adult

438 size to temperatures experienced during the early larval and pupal stages were less

439 consistent. Only eight of the 20 models had a significant change in adult size in relation to

440 changes in temperature during the early larval stage and eight models had significant

441 changes in adult size in the pupal stage, with both having a mix of increases and decreases

442 in size with increasing temperatures. The percentage changes in adult size per increase in °C

443 during each immature stage are given in SI Table 5, and detailed individual model results are

444 in the supplementary information (SI tables 3 and 4).

445

446 3.4 Temperature-size responses: multi-species analysis

447

448 The influence of temperature during the immature stages on adult size for each species

449 were compared in two ways: using percentage change in size from all species and using only

450 those with significant individual models (SI Table 5). There was little difference in the results

451 between the two methods and, therefore, the results presented here are for species with

452 significant models only. There was no significant difference in the mean percentage change

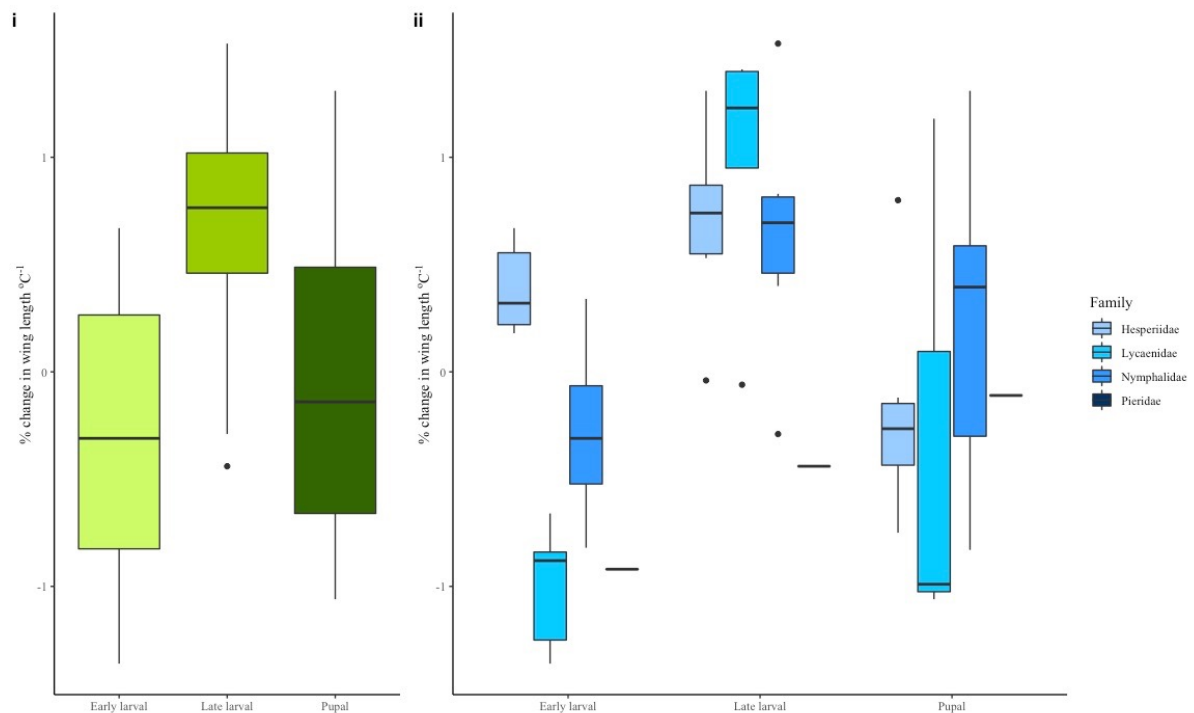
453 in adult size between species in different size categories or between species that

454 overwintered in different life history stages ($p > 0.05$). There were no significant differences

455 in mean percentage change in adult size between species occurring in different habitat
456 types for the early and late larval stages, but there was for the pupal stage ($F=3.649$, $df=3$
457 and 14, $p=0.0392$), with a difference between those in a woodland habitat and those in
458 grassland habitats ($p=0.0477$).

459

460 There was a significant difference in percentage change in adult size according to the three
461 developmental stages for species with significant individual models ($F=12.21$, $df=2$ and 55,
462 $p<0.001$), with differences between percentage changes per °C in the late larval stage and
463 both the early larval and pupal stages ($p<0.01$; Fig. 6). On average, forewing length
464 increased by 0.69% per °C increase in temperature during the late larval stage ($SE=0.13$),
465 decreased by 0.29% per °C in the early larval stage ($SE=0.14$), and decreased by 0.02% per °C
466 in the pupal stage ($SE=0.17$). Additionally, there were significant differences in percentage
467 change in adult size per °C temperature increase in the early larval stage between species
468 from different families ($F=15.74$, $df=3$ and 16, $p<0.001$), with differences between the
469 Hesperidae and all other families, and the Lycaenidae and the Nymphalidae ($p<0.05$). On
470 average, there was a 0.39% increase in average forewing length per °C temperature increase
471 in the early larval stage for the Hesperidae, a 0.99% decrease in size per °C for the
472 Lycaenidae, and a 0.28% decrease in size per °C in the Nymphalidae (Fig. 6). A two-way
473 ANOVA to test for differences in percentage changes in adult size between stages and
474 families also found a significant interaction between life stage and family ($F=3.004$, $df=6$ and
475 46, $p=0.0146$). There is a large difference in responses to temperatures between larval
476 stages for the Lycaenidae (Fig. 6); on average, there is a large increase in adult size per °C
477 temperature increase in the late larval stage (0.99%), but a large decrease in adult size per
478 °C in the early larval stage (-0.99%).



479

480 FIGURE 6. Boxplots of percentage change in adult size per °C change during (i) the early
481 larval, late larval and pupal stages and (ii) for species grouped by family within each stage.

482 NB: There is only one species of Pieridae with a significant response (*Pieris napi*).

483

484

485 For the linear mixed effects models, various models were tested using combinations of
486 factors for the fixed effects, starting with a simple model and becoming more complicated.

487 Family was given priority in selection of factors as the above analyses showed there were
488 significant differences in responses between families. The model with the lowest AIC value

489 was Average forewing length (Ln) ~ Early larval temperature + Late larval temperature +

490 Pupal temperature + (1|Family) (AIC=-20579). For the species where sex could be

491 determined, the model which was most significant was Average forewing length (Ln) ~ Early

492 larval temperature + Late larval temperature + Pupal temperature + (1|Sex) + (1|Family)

493 (AIC=-15324). In both models (for all species and those which can be sexed), family

494 explained the highest proportion of variance in the results (SI Table 6).

495

496 4 DISCUSSION

497

498 The huge effort currently underway to digitise natural history collections (NHCs) will make
499 museum specimens and their associated collecting data accessible to scientists all over the
500 globe. A major reason for this mass digitisation effort is to accelerate their usage for global
501 change research (Hedrick *et al.* 2020). There is now an increasing need for ecologists and
502 museum scientists to collaborate with computer vision (CV) scientists in order to help make
503 sense of these massive datasets. Our study is among the first to show that CV can accurately
504 measure phenotypic data from very large digitised NHC datasets in order to test biotic
505 response to climate change hypotheses.

506

507 We show that Mothra accurately measures multiple phenotypic aspects of butterfly
508 specimens (Figs. 1-3). It can also tell whether a specimen is pinned ventrally or dorsally, and
509 its sex (for species where sexes are detectable by eye). While each of these attributes can be
510 measured manually from images, the time involved would be immense: manual
511 measurements of all imaged butterfly specimens (n=184,533) by a single person would take
512 >3,000 hours (or ~2 years, assuming regular working hours, and only forewing length
513 measurements). Using Mothra, we were able to run all specimens in under one week by
514 performing 10 analyses in parallel on a computer cluster, and could have reduced the time
515 further by running more analyses in parallel (e.g., 50 analyses in parallel would have
516 reduced the time to a mere 30 hours and remained within the capacity of the current NHM
517 cluster: 96 CPUs, 2TB RAM, Centos 7 OS).

518

519 CV applied to digitised NHCs will become a common tool in ecology and evolution research
520 (Lürig *et al.* 2021). CV will help scientists uncover unknown aspects of the biology and
521 morphology of species, but also to confirm/test hypotheses or suspected patterns based on
522 previous research using manual measurements. For example, we test hypotheses that were
523 formulated based on recent studies on temperature-size responses using manual
524 measurements (Fenberg *et al.* 2016; Wilson *et al.* 2019). For most species with a significant
525 temperature-size response (14/17), adult size increases with increasing temperature during
526 the late larval stage (Fig. 6), which is consistent with these studies. While some species did
527 not show this response, there were no species, sexes or generations that showed the
528 reverse response. This pattern, while suspected, is now clearer thanks to the application of
529 CV to many more specimens and species. We suggest that this is because a higher volume
530 and/or quality of food is available during years with warmer temperatures during the late
531 larval stages. Therefore, late larval stage individuals can reach optimum growth rates when
532 food quality and quantity are plentiful, resulting in larger adults (Suhling *et al.* 2015).
533 However, the optimum temperature for growth and the highest rate of growth will vary
534 between species, sexes, and generations.

535

536 As expected, different generations did not respond in the same way to temperature (Wilson
537 *et al.* 2019). For the three bivoltine species, each responded in the first generation but not
538 in the second (*P. bellargus*, *A. urticae*, and *P. napi*). The different responses between
539 generations were expected as the larvae of each generation experience different
540 environmental conditions, which can affect adult body size (Horne *et al.* 2017). In addition,
541 different temperature-size responses between the sexes can also occur (Fenberg *et al.* 2016;
542 Wilson *et al.* 2019). Of the 15 species in which the sexes were analysed separately, males

543 had a significant temperature-size response in eight species and females responded in five
544 species (three species had a significant response in both sexes), and there was no response
545 from either sex for five species. In all but one of the species with significant results, the
546 responses to temperature differed between males and females (i.e., the significance or
547 direction of the temperature response was different in at least one developmental stage).

548

549 In the multi-species analyses, family explained the highest proportion of variance. Although
550 significant responses to temperature in the late larval stage were always positive, the
551 magnitude was greatest for Lycaenidae (Fig. 6). The response to early larval stage
552 temperatures shows the clearest differences between families: all Hesperidae species with
553 significant models showed an increase in adult size with increasing temperature and
554 Lycaenidae species showing a decrease in adult size with increasing temperature.

555 Meanwhile, the species analysed within the Pieridae showed very little response; the only
556 significant response was a decrease in adult size of generation one male *P. napi* with
557 increasing temperature in the early larval stage. Overall, the Lycaenidae show the largest
558 variation in responses to temperature between the immature stages, with a large increase
559 in adult size (0.99% per °C on average) with increasing temperatures in the late larval stage
560 and a large decrease in adult size (-0.99% per °C on average) with increasing temperature in
561 the early larval stage. In the pupal stage, there was a range of positive and negative
562 responses within each family. There are also some differences in response between species
563 from different habitat types, particularly to temperature during the pupal stage, which may
564 be due to differences in the microclimates within the habitats experienced by each stage (SI
565 Fig. 1).

566

567 We also can now confirm that females are the larger sex for most species of British
568 butterflies. While this is not particularly surprising given that female biased sexual-size
569 dimorphism (SSD) is commonly reported across insect species (Teder 2014), our study
570 represents the largest test of this phenomenon in terms of sample sizes. All species of
571 HesperIIDae and Nymphalidae have female biased SSD, but at least five species of
572 Lycaenidae and two species of Pieridae have male biased SSD (Fig. 5). Interestingly, four of
573 the Lycaenidae species with male biased SSD are in the subfamily Polyommatainae. In these
574 species, there is also a strong colour dimorphism between the sexes. While the reason some
575 species of this subfamily have male biased SSD requires more research, we can make some
576 inferences based on their natural history. In most species of insects, the males emerge
577 earlier than females, termed protandry (Teder *et al.* 2021). In Polyommatainae, males
578 actively compete and swarm upon freshly emerged females to mate (e.g., in *P. bellargus*;
579 Thomas & Lewington 2014). Larger males may therefore be at a competitive advantage and
580 promote male biased SSD. While the causes of SSD in insects is an ongoing debate and are
581 likely to vary among taxa, our research shows that the direction and strength of
582 temperature-size responses often varies by sex. Thus, the magnitude of SSD may increase,
583 decrease, or stay the same with increasing temperature.

584

585 Clearly, temperature size responses in insects are a complex interaction between many
586 different ecological, geographic, environmental, life history, evolutionary, and historical
587 variables. While the use of natural history collections can give us valuable clues to how
588 temperature affects size, and CV can greatly accelerate data collection and analysis, there
589 will always be a need to conduct field, laboratory, and long-term monitoring studies to
590 better understand the complexities of how insects will respond to climate change.

591

592 **Acknowledgements**

593

594 We thank the iCollections team (NHM) for capturing the images and data, Paul Ward (NHM)
595 for providing server access to the images, Robert Foster (NHM) for access to and training on
596 the HPC cluster, and James Durrant for developing an early wing measurement prototype.

597 We thank Gary Fisher, Graham Wilson and Hannah O'Sullivan for their help with the image
598 analysis, and Dennis Feng, Sera Yang, Teddy Tran and Théo Bodrito for their work on

599 preliminary versions of Mothra. This work was supported by the Natural Environmental

600 Research Council (grant number NE/L002531/1), and in part by the Gordon and Betty Moore

601 Foundation (Grant GBMF3834) and by the Alfred P. Sloan Foundation (Grant 2013-10-27) to

602 the University of California, Berkeley.

603

604

605 **Author Contributions**

606 PBF, RJW, BWP, and SJB conceived of the ideas for the paper. AdS and SvdW developed

607 Mothra and wrote the accompanying methods section. BWP and PBF analysed the Mothra

608 outputs. LS and RJW performed manual measurements. RJW performed all temperature size

609 analyses. RJW and PBF wrote most of the paper with helpful comments and edits from all

610 co-authors.

611

612 Data availability statement: all data will be archived on Zenodo

613 REFERENCES

- 614 Ariño, A.H. (2010) Approaches to estimating the universe of natural history collections data.
615 *Biodiversity Informatics*, **7**, 81-92.
- 616 Baar, Y., Friedman, A.L.L., Meiri, S. & Scharf, I. (2018) Little effect of climate change on body
617 size of herbivorous beetles. *Insect Science*, **25**, 309-316.
- 618 Bjerge, K., Nielsen, J.B., Sepstrup, M.V., Helsing-Nielsen, F. & Høye, T.T. (2021) An
619 automated light trap to monitor moths (Lepidoptera) using computer vision-based
620 tracking and deep learning. *Sensors*, **21**, 343.
- 621 Bowden, J.J., Eskildsen, A., Hansen, R.R., Olsen, K., Kurle, C.M. & Høye, T.T. (2015) High-
622 Arctic butterflies become smaller with rising temperatures. *Biology Letters*, **11**,
623 20150574.
- 624 Brooks, S.J., Self, A., Powney, G.D., Pearse, W.D., Penn, M. & Paterson, G.L. (2017) The
625 influence of life history traits on the phenological response of British butterflies to
626 climate variability since the late-19th century. *Ecography*, **40**, 1152-1165.
- 627 Buslaev, A., Iglovikov, V.I., Khvedchenya, E., Parinov, A., Druzhinin, M. & Kalinin, A.A. (2020)
628 Albumentations: fast and flexible image augmentations. *Information*, **11**, 125.
- 629 Davies, W.J. (2019) Multiple temperature effects on phenology and body size in wild
630 butterflies predict a complex response to climate change. *Ecology*, **100**, e02612.
- 631 Deng, J., Dong, W., Socher, R., Li, L.-J., Li, K. & Fei-Fei, L. (2009) Imagenet: A large-scale
632 hierarchical image database. *2009 IEEE conference on computer vision and pattern
633 recognition*, pp. 248-255. Ieee.
- 634 DeVries, T. & Taylor, G.W. (2017) Improved regularization of convolutional neural networks
635 with cutout. *arXiv preprint arXiv:1708.04552*.
- 636 Ewers-Saucedo, C., Allspach, A., Barilaro, C., Bick, A., Brandt, A., Fiege, D., Fütting, S.,
637 Hausdorf, B., Hayer, S. & Husemann, M. (2021) Natural history collections
638 recapitulate 200 years of faunal change. *Royal Society open science*, **8**, 201983.
- 639 Fenberg, P.B., Self, A., Stewart, J.R., Wilson, R.J. & Brooks, S.J. (2016) Exploring the universal
640 ecological responses to climate change in a univoltine butterfly. *Journal of Animal
641 Ecology*, **85**, 739-748.
- 642 Harris, C.R., Millman, K.J., van der Walt, S.J., Gommers, R., Virtanen, P., Cournapeau, D.,
643 Wieser, E., Taylor, J., Berg, S. & Smith, N.J. (2020) Array programming with NumPy.
644 *Nature*, **585**, 357-362.
- 645 He, K., Zhang, X., Ren, S. & Sun, J. (2016) Deep residual learning for image recognition.
646 *Proceedings of the IEEE conference on computer vision and pattern recognition*, pp.
647 770-778.
- 648 Hedrick, B.P., Heberling, J.M., Meineke, E.K., Turner, K.G., Grassa, C.J., Park, D.S., Kennedy,
649 J., Clarke, J.A., Cook, J.A. & Blackburn, D.C. (2020) Digitization and the future of
650 natural history collections. *BioScience*, **70**, 243-251.
- 651 Horne, C.R., Hirst, A.G. & Atkinson, D. (2015) Temperature-size responses match latitudinal-
652 size clines in arthropods, revealing critical differences between aquatic and
653 terrestrial species. *Ecology Letters*, **18**, 327-335.
- 654 Horne, C.R., Hirst, A.G. & Atkinson, D. (2017) Seasonal body size reductions with warming
655 covary with major body size gradients in arthropod species. *Proceedings of the Royal
656 Society B: Biological Sciences*, **284**, 20170238.
- 657 Howard, J. & Gugger, S. (2020) Fastai: a layered API for deep learning. *Information*, **11**, 108.

- 658 Høye, T.T., Ärje, J., Bjerger, K., Hansen, O.L., Iosifidis, A., Leese, F., Mann, H.M., Meissner, K.,
659 Melvad, C. & Raitoharju, J. (2021) Deep learning and computer vision will transform
660 entomology. *Proceedings of the National Academy of Sciences*, **118**.
- 661 Hsiang, A.Y., Brombacher, A., Rillo, M.C., Mleneck-Vautravers, M.J., Conn, S., Lordsmith, S.,
662 Jentzen, A., Henehan, M.J., Metcalfe, B. & Fenton, I.S. (2019) Endless Forams:>
663 34,000 modern planktonic foraminiferal images for taxonomic training and
664 automated species recognition using convolutional neural networks.
665 *Paleoceanography and Paleoclimatology*, **34**, 1157-1177.
- 666 Hunter, J.D. (2007) Matplotlib: A 2D graphics environment. *Computing in Science &*
667 *Engineering*, **9**, 90-95.
- 668 Johnson, K.G., Brooks, S.J., Fenberg, P.B., Glover, A.G., James, K.E., Lister, A.M., Michel, E.,
669 Spencer, M., Todd, J.A. & Valsami-Jones, E. (2011) Climate change and biosphere
670 response: unlocking the collections vault. *BioScience*, **61**, 147-153.
- 671 Kharouba, H.M., Lewthwaite, J.M., Guralnick, R., Kerr, J.T. & Vellend, M. (2019) Using insect
672 natural history collections to study global change impacts: challenges and
673 opportunities. *Philosophical Transactions of the Royal Society B*, **374**, 20170405.
- 674 Kingsolver, J.G., Arthur Woods, H., Buckley, L.B., Potter, K.A., MacLean, H.J. & Higgins, J.K.
675 (2011) Complex life cycles and the responses of insects to climate change. Oxford
676 University Press.
- 677 Lürig, M.D., Donoughe, S., Svensson, E.I., Porto, A. & Tsuboi, M. (2021) Computer vision,
678 machine learning, and the promise of phenomics in ecology and evolutionary
679 biology. *Frontiers in Ecology and Evolution*, **9**, 148.
- 680 MacLean, H.J., Kingsolver, J.G. & Buckley, L.B. (2016) Historical changes in thermoregulatory
681 traits of alpine butterflies reveal complex ecological and evolutionary responses to
682 recent climate change. *Climate Change Responses*, **3**, 1-10.
- 683 McAllister, C.A., McKain, M.R., Li, M., Bookout, B. & Kellogg, E.A. (2019) Specimen-based
684 analysis of morphology and the environment in ecologically dominant grasses: the
685 power of the herbarium. *Philosophical Transactions of the Royal Society B*, **374**,
686 20170403.
- 687 Meineke, E.K., Davies, T.J., Daru, B.H. & Davis, C.C. (2019) Biological collections for
688 understanding biodiversity in the Anthropocene. *Philosophical Transactions of the*
689 *Royal Society B*, **374**, 20170386.
- 690 Mothra Team (2020): <https://gitlab.com/mothra/mothra-data>
691 Mothra Team (2021): <https://github.com/machine-shop/mothra/>
- 692 Nelson, G. & Ellis, S. (2019) The history and impact of digitization and digital data
693 mobilization on biodiversity research. *Philosophical Transactions of the Royal Society*
694 *B*, **374**, 20170391.
- 695 Otsu, N. (1979) A threshold selection method from gray-level histograms. *IEEE transactions*
696 *on systems, man, and cybernetics*, **9**, 62-66.
- 697 Paszke, A., Gross, S., Massa, F., Lerer, A., Bradbury, J., Chanan, G., Killeen, T., Lin, Z.,
698 Gimelshein, N. & Antiga, L. (2019) Pytorch: An imperative style, high-performance
699 deep learning library. *Advances in neural information processing systems*, **32**, 8026-
700 8037.
- 701 Paterson, G., Albuquerque, S., Blagoderov, V., Brooks, S., Cafferty, S., Cane, E., Carter, V.,
702 Chainey, J., Crowther, R. & Douglas, L. (2016) iCollections—Digitising the British and
703 Irish Butterflies in the Natural History Museum, London. *Biodiversity Data Journal*, **4**,
704 e9559.

- 705 Price, Benjamin W., & Fenberg, Phillip B. (2021). Results of Mothra analysis of all iCollections
706 butterflies [Data set]. Zenodo. <https://doi.org/10.5281/zenodo.5759759>
- 707 Ronneberger, O., Fischer, P. & Brox, T. (2015) U-net: Convolutional networks for biomedical
708 image segmentation. *International Conference on Medical image computing and*
709 *computer-assisted intervention*, pp. 234-241. Springer.
- 710 Sheridan, J.A. & Bickford, D. (2011) Shrinking body size as an ecological response to climate
711 change. *Nature Climate Change*, **1**, 401-406.
- 712 Smith, L.N. (2018) A disciplined approach to neural network hyper-parameters: Part 1--
713 learning rate, batch size, momentum, and weight decay. *arXiv preprint*
714 *arXiv:1803.09820*.
- 715 Suhling, F., Suhling, I. & Richter, O. (2015) Temperature response of growth of larval
716 dragonflies—an overview. *International Journal of Odonatology*, **18**, 15-30.
- 717 Svoboda, E. (2020) Artificial intelligence is improving the detection of lung cancer. *Nature*,
718 **587**, S20-S22.
- 719 Teder, T. (2014) Sexual size dimorphism requires a corresponding sex difference in
720 development time: A meta-analysis in insects. *Functional Ecology*, **28**, 479-486.
- 721 Teder, T., Kaasik, A., Taits, K. & Tammaru, T. (2021) Why do males emerge before females?
722 Sexual size dimorphism drives sexual bimaturism in insects. *Biological Reviews*.
- 723 Thomas, J. & Lewington, R. (2014) *The butterflies of Britain and Ireland*. Bloomsbury
724 Publishing.
- 725 Tseng, M., Kaur, K.M., Soleimani Pari, S., Sarai, K., Chan, D., Yao, C.H., Porto, P., Toor, A.,
726 Toor, H.S. & Fograscher, K. (2018) Decreases in beetle body size linked to climate
727 change and warming temperatures. *Journal of Animal Ecology*, **87**, 647-659.
- 728 Van der Walt, S., Schönberger, J.L., Nunez-Iglesias, J., Boulogne, F., Warner, J.D., Yager, N.,
729 Gouillart, E. & Yu, T. (2014) scikit-image: image processing in Python. *PeerJ*, **2**, e453.
- 730 Virtanen, P., Gommers, R., Oliphant, T.E., Haberland, M., Reddy, T., Cournapeau, D.,
731 Burovski, E., Peterson, P., Weckesser, W. & Bright, J. (2020) SciPy 1.0: fundamental
732 algorithms for scientific computing in Python. *Nature methods*, **17**, 261-272.
- 733 Wilson, R. (2021) Disentangling the effects of ecology and life history on ectothermic
734 temperature-size responses. University of Southampton.
- 735 Wilson, R.J., Fenberg, P.B., Brooks, S.J., van der Walt, S., Feng, D., & Price, B.W.
736 (2020). iCollections butterfly images selected for automated measurement.
737 [Data set]. Zenodo. <https://doi.org/10.5281/zenodo.3732132>
- 738 Wilson, R.J., Brooks, S.J. & Fenberg, P.B. (2019) The influence of ecological and life history
739 factors on ectothermic temperature–size responses: Analysis of three Lycaenidae
740 butterflies (Lepidoptera). *Ecology and Evolution*, **9**, 10305-10316.
- 741 Wonglersak, R., Fenberg, P.B., Langdon, P.G., Brooks, S.J. & Price, B.W. (2020) Temperature-
742 body size responses in insects: a case study of British Odonata. *Ecological*
743 *Entomology*, **45**, 795-805.
- 744 Zhang, Z., Liu, Q. & Wang, Y. (2018) Road extraction by deep residual u-net. *IEEE Geoscience*
745 *and Remote Sensing Letters*, **15**, 749-753